AGU ADVANCING EARTH AND SPACE SCIENCE

Water Resources Research

RESEARCH ARTICLE
10.1029/2020WR027495

Tropical Montane Forest Conversion Is a Critical Driver for Sediment Supply in East African Catchments

Jaqueline Stenfert Kroese[1,2], Suzanne R. Jacobs[3], Wlodek Tych[1], Lutz Breuer[3,4], John N. Quinton[1], and Mariana C. Rufino[1,2]

[1]Lancaster Environment Centre, Lancaster University, Lancaster, Lancashire, United Kingdom, [2]Centre for International Forestry Research (CIFOR), c/o World Agroforestry Centre, Nairobi, Kenya, [3]Centre for International Development and Environmental Research (ZEU), Justus Liebig University Giessen, Giessen, Germany, [4]Institute for Landscape Ecology and Resources Management (ILR), Justus Liebig University Giessen, Giessen, Germany

Key Points:
- Agricultural catchments generated six times more suspended sediment yield than a forested catchment
- Land use change toward agriculture shifted the dominant water pathways from deep subsurface to shallow subsurface flow and surface runoff
- Delayed sediment responses were observed in a smallholder agriculture catchment, in contrast to fast responses in a forested catchment

Supporting Information:
- Supporting Information S1

Correspondence to:
J. Stenfert Kroese,
j.stenfertkroese@lancaster.ac.uk

Citation:
Stenfert Kroese, J., Jacobs, S. R., Tych, W., Breuer, L., Quinton, J. N., & Rufino, M. C. (2020). Tropical montane forest conversion is a critical driver for sediment supply in East African catchments. *Water Resources Research*, *56*, e2020WR027495. https://doi.org/10.1029/2020WR027495

Received 11 MAR 2020
Accepted 5 SEP 2020
Accepted article online 16 SEP 2020

Abstract Land use change is known to affect suspended sediment fluxes in headwater catchments. There is however limited empirical evidence of the magnitude of these effects for montane catchments in East Africa. We collected a unique 4-year high-frequency data set and assessed seasonal sediment variation, water pathways, and sediment response to hydrology in three catchments under contrasting land use in the Mau Forest Complex, Kenya's largest tropical montane forest. Annual suspended sediment yield was significantly higher in a smallholder agriculture-dominated catchment (131.5 ± 90.6 t km^{-2} yr^{-1}) than in a tea-tree plantation catchment (42.0 ± 21.0 t km^{-2} yr^{-1}) and a natural forest catchment (21.5 ± 11.1 t km^{-2} yr^{-1}) ($p < 0.05$). Transfer function models showed that in the natural forest and the tea-tree plantations subsurface flow pathways delivered water to the stream, while in the smallholder agriculture shallow subsurface and surface runoff were dominant. There was a delayed sediment response to rainfall for the smallholder agriculture and the tea-tree plantations. A slow depletion in sediment supply suggests that the wider catchment area supplies sediment, especially in the catchment dominated by smallholder farming. In contrast, a fast sediment response and depletion in sediment supply in the natural forest suggests a dominance of temporarily stored and nearby sediment sources. This study shows that the vegetation cover of a forest ecosystem is very effective in conserving soil, whereas catchments with more bare soil and poor soil conservation practices generated six times more suspended sediment yield. Catchment connectivity through unpaved tracks is thought to be the main explanation for the difference in sediment yield.

1. Introduction

The conversion of native ecosystems to agriculture leads to the degradation of soil properties (Githui et al., 2009; Morgan, 2005; Owuor et al., 2018), which can increase soil erosion rates (Bruijnzeel, 2004). Soil erosion does not only deplete fertile topsoil from agricultural land but also leads to water quality deterioration caused by an increase in fine suspended sediments (Brown et al., 1996; Horowitz, 2008; Quinton et al., 2001). Hence, suspended sediment physically affects the fluvial network, (Owens et al., 2005) polluting drinking water for communities, livestock and wildlife, and impacting downstream water reservoirs and hydropower generation because of the accumulation of the sediments (Foster et al., 2012; Mogaka, 2006; Wangechi et al., 2015). Additionally, pollutants such as pesticides (Brown et al., 1996) and nutrients (phosphorus or nitrogen) (Fraser et al., 1999; Horowitz, 2008; Quinton et al., 2001) can be attached to sediments and can harm aquatic biota (Gellis & Mukundan, 2013; Kemp et al., 2011; Owens et al., 2005). The increase in nutrient concentrations can result in eutrophication of water bodies (Foy & Bailey-Watts, 1998; Hilton et al., 2006; Mogaka, 2006).

Land use change in catchments with strong connectivity between sediment sources and streams can abruptly increase sediment supply to the fluvial system (Fryirs, 2013). There may be multiple sediment source areas, such as hillslope soils (Didoné et al., 2014; Minella et al., 2008), gullies (Fan et al., 2012; Minella et al., 2008; Poesen et al., 2003), riverbanks (Lefrançois et al., 2007; Trimble & Mendel, 1995), and unpaved tracks (Minella et al., 2008; Ramos-Scharrón & Thomaz, 2016; Ziegler et al., 2001). Unraveling sediment dynamics is complex and requires continuous high-frequency monitoring because suspended sediment concentrations change rapidly throughout individual storms (De Girolamo et al., 2015; Sun et al., 2016;

Vercruysse et al., 2017). Alternatively, turbidity observations can be used as a surrogate to determine in-stream suspended sediment concentrations, which allow for establishing continuous in situ suspended sediment data sets, even for remote sites (Lewis, 1996; Minella et al., 2018; Ziegler et al., 2014).

Streams in montane headwaters are major contributors to suspended sediment yield because of the steep terrain that leads to a strong hillslope to channel connectivity (Grangeon et al., 2012; Morris, 2014; Wohl, 2006). Significant increases in suspended sediment yield can be expected from tropical montane headwater catchments, which are heavily affected by deforestation followed by cultivation of erosion prone areas, often without soil conservation measures (Ramos-Scharrón & Thomaz, 2016; Wohl, 2006). Land use change may impact catchment hydrology and runoff mechanisms in the tropics (Muñoz-Villers & McDonnell, 2013; Ogden et al., 2013), which are key processes determining sediment yields.

In East Africa, land use change in tropical montane forests is mainly driven by scarcity of arable land (Pellikka et al., 2004) with the most fertile lands located in the proximity of natural ecosystems (Krhoda, 1988). The Mau Forest Complex exemplifies this case, with one quarter of the forest converted to agricultural land over the last four decades (Brandt et al., 2018), in addition to the clearances at the beginning of the twentieth century to establish commercial tea plantations (Binge, 1962). Due to its location in the highlands of Kenya, the Mau forest is a critical catchment area for the country; it is the headwater to twelve rivers, one of which is the Sondu River, a tributary of Lake Victoria (Mogaka, 2006; UNEP, 2005).

Eutrophication and sedimentation are major environmental problems affecting Lake Victoria, where sediments are estimated to accumulate at a rate of 2.3 mm yr^{-1} (Verschuren et al., 2002). Although authorities in Kenya acknowledge the need to reduce sediment pollution, the linkages between land use change and changes in sediment dynamics in the headwater catchments are not well quantified (Nyssen et al., 2004; Vanmaercke et al., 2010, 2014). There are limited data on sediment export for montane catchments in Sub-Saharan Africa in general and in East Africa in particular (Ntiba et al., 2001; Walling & Webb, 1996). Clearly, this is a significant gap in our knowledge of these environments that requires empirical measurements to address it. Not only will these measurements improve our understanding of these underresearched environments, but they will also assist in the development of targeted soil and water conservation strategies to disconnect sediment source areas in the upper catchments of the Mau Forest from the fluvial system and downstream environments, including Lake Victoria.

The overall aim of this study was to elucidate the spatial and temporal dynamics of suspended sediment and to quantify suspended sediment loads in tropical montane streams under contrasting land uses using a 4 year high-temporal resolution data set. The main objectives were (a) to quantify rainfall, streamflow, and suspended sediment transport dynamics, (b) to compare the seasonal responses in suspended sediment yield, (c) to assess the timing of the response of suspended sediment to rainfall and discharge, and (d) to improve our understanding of the dominant water flow pathways.

2. Materials and Methods

2.1. Catchment Characteristics and Site Description

The three catchments studied are located in the headwaters of the Sondu River Basin (3,470 km^2) in the Western Highlands of Kenya (Figure 1). Each catchment is dominated by a distinct land use: (1) natural forest (NF; 35.9 km^2), (2) smallholder agriculture (SHA; 27.2 km^2), and (3) tea-tree plantations (TTPs; 33.3 km^2). The Sondu River drains into Lake Victoria, which is the second largest fresh water lake in the world, an important water and economic resource for five countries and one source of the Nile River.

The three catchments (Table 1) are characterized by steep hillslopes with a maximum slope gradient of 72% in the NF catchment. The streams are mostly first- and second-order perennial streams that merge together to form the River Sondu (a sixth-order stream). The rainy seasons are bimodal with a long rainy season between March and June and a short rainy season between October and December with a continued intermediate rainy season between the two wet seasons. Mean annual precipitation is 1,988 $\pm$ 328 mm (period 1905–2014) with rainfall peaks in April and May (>260 mm $month^{-1}$). January and February (<95 mm $month^{-1}$) are the driest months.

The NF catchment is located in the South-West Mau block of the Mau Forest Complex. The Mau Forest is an afromontane mixed forest dominated by indigenous broad-leafed evergreen trees and shrubs with

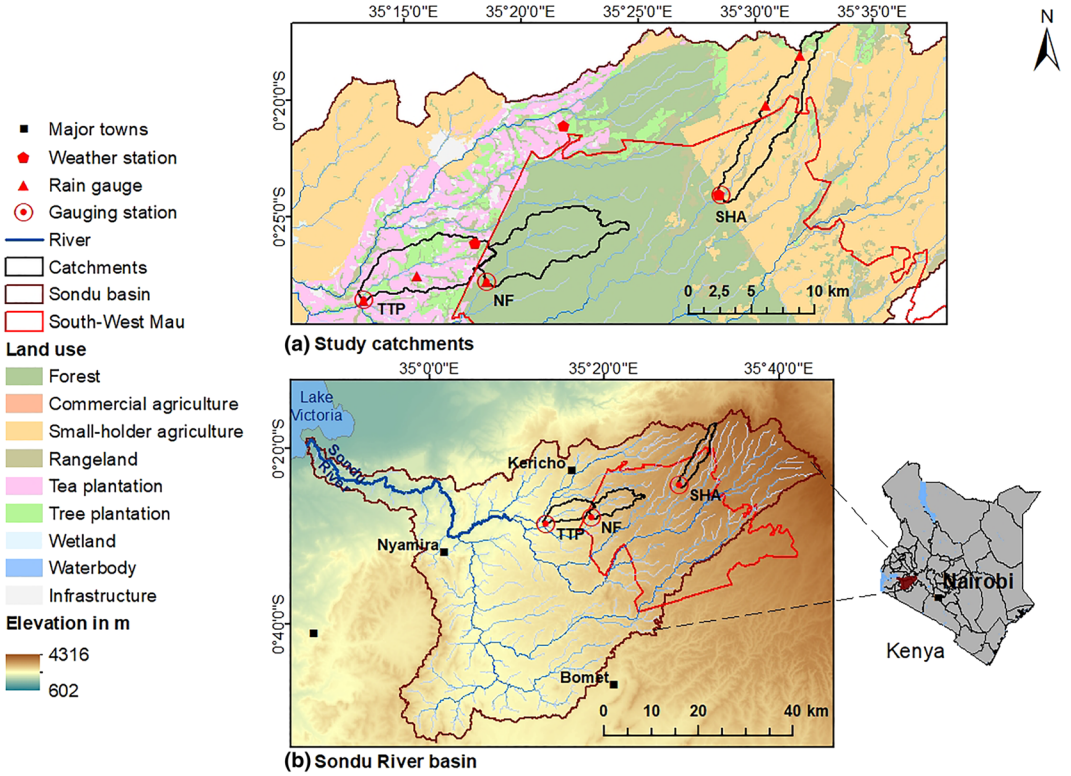

Figure 1. Overview of the (a) study catchments: tea-tree plantations (TTP), natural forest (NF), and the smallholder agriculture (SHA), showing locations of gauging and weather stations, tipping bucket rain gauges and land use in the (b) Sondu River Basin and its outlet to Lake Victoria (SRTM digital elevation model 30 m resolution; USGS, 2000) in Western Kenya.

a complex vegetation pattern. Riparian forests with a mixture of indigenous vegetation are present throughout the catchment. The NF catchment is characterized by high infiltration rates with the occurrence of shallow to deeper subsurface water pathways, whereas the TTP and the SHA catchments have lower infiltration rates with a dominance of surface runoff (Jacobs, Timbe, et al., 2018; Owuor et al., 2018) (Table 1).

In the SHA catchment, subsistence farmers grow maize interspersed with beans, potatoes, millet, and cabbage on small farms (~1 ha). Small-scale tea plantations, eucalyptus (*Eucalyptus* spp.), cypress (*Cypressus* spp.), and pine (*Pinus* spp.) woodlots are interspersed with crop fields and grazing land (Table 1). A combination of hand weeding, hoeing, and herbicides is used for weed control. Bamboo (*Bambusa* spp.) is generally found around natural springs. The whole catchment is connected by a dense network of unpaved tracks either bare or sparsely covered by grass; stream crossings rarely have bridges. The heavily traveled unpaved tracks have commonly become eroded gullies (Figures 2a and 2b), which run down the slope to rivers, connecting surface runoff from surrounding fields with the stream network (Figures 2c–2e). Cattle entrance points to the stream are generally highly disturbed and have degraded riverbanks (Figures 2d–2f). The natural riparian vegetation is in many areas replaced by eucalyptus woodlots or small bushes. In some places, riparian wetlands are found.

The TTP catchment has tea fields alternated with *Eucalyptus* spp. and *Cypress* spp. woodlots that are used for fuelwood at the tea factories. Some of the tea companies use mulch and rows of oat grass between rows of tea to control soil erosion during the establishment of new tea bushes. Herbicides are commonly used to control weeds. Cover crops with mature tea trees during the establishment of a new tea crop, terracing and sited cut-off drains are also used within the catchment to control soil erosion. The catchment is covered by a network of well-maintained paved and unpaved roads, linked to drainage systems, such as open culverts along the

Table 1
Physical Characteristics of the Three Catchments Under Different Land Use Natural Forest, Tea-Tree Plantations, and Smallholder Agriculture in the South-West Mau, Kenya

	Natural forest	Tea-tree plantations	Smallholder agriculture
Outlet coordinates[a]	35°18′32.0472″E 0°27′47.592″S	35°13′17.22″E 0°28′34.9176″S	35°28′31.7316″E 0°24′4.0248″S
Area (km^2)	35.9	33.3	27.2
Elevation range (m a.s.l.)	1,968–2,385	1,788–2,141	2,389–2,691
Mean slope ± SD (%)	15.7 ± 8.4	12.4 ± 7.6	11.6 ± 6.7
Basin order (Strahler)	2	2	2
Drainage density (km $km^{-2)}$	0.48	0.42	0.64
Soil infiltration rate (mm hr^{-1})[b]	760 ± 500	430 ± 290	401 ± 211
Geology[c]	Igneous rock (volcanic) (100%)	Igneous rock (volcanic) (100%)	Igneous rock (volcanic) (72%) and pyroclastic (28%)
Dominant soils[c]	Humic Nitisols (100%)	Humic Nitisols (100%)	Humic Nitisols (72%) and mollic Andosols (28%)
Vegetation	Afromontane mixed forest, grassland, bamboo, broad-leafed evergreen trees, and shrubs	Tea plantations with woodlots of *Eucalyptus* spp., *Cypress* spp., and *Pinus* spp.	Perennial and annual crops (maize interspersed with beans, potatoes, millet, cabbage, and onions), woodlots, and grassland
Riparian vegetation	Forest vegetation	>30 m buffer with indigenous vegetation	Degraded riparian vegetation and eucalyptus woodlots

[a]WGS 1984 UTM Zone 36S. [b]Owuor et al. 2018 [c]KENSOTER geology data from the soil and terrain database for Kenya (KENSOTER) Version 2.0.

roads that connect them to the streams. The riparian vegetation includes a mix of indigenous tree species that cover densely the ground and form a buffer of approximately 30 m (Table 1).

The study area is composed of folded volcanics from the early Miocene times. Porphyritic phonolites, a member of the sequence of basic and intermediate lavas (igneous rocks) are predominant in the study area (Binge, 1962), where pyroclastic rocks cover the upper part of the catchment (ISRIC, 2007). The study area comprises well-drained, very deep (>1.8 m) dark-red and dark-brown loamy soils (Sombroek et al., 1982), with moderate to high amounts of organic matter under the forest cover (Dunne, 1979).

2.2. Automated Hydrological and Sediment Monitoring

This study uses a 4 year data set (January 2015 to December 2018) on rainfall, discharge, and turbidity with a 10 min resolution (Figure 1). A radar sensor (VEGAPULS WL61, VEGA Grieshaber KG, Schiltach, Germany) collected continuous water level measurements. Water level ("stage") was used to determine stream discharge based on a site-specific second-order polynomial stage-discharge relationship (Jacobs, Weeser, et al., 2018). The calibration was checked over a wide range of stream flows using salt-dilution gauging (Shaw et al., 2011), an Accoustic Doppler Velocimeter (ADV; FlowTracker, SonTek, San Diego CA, USA) or an Acoustic Doppler Current Profiler (ADCP; RiverSurveyor S5, SonTek, San Diego, USA) depending on river size and discharge (Jacobs, Weeser, et al., 2018). Specific discharge (mm day^{-1}) was determined by integrating instantaneous discharge taken at 10 min intervals over a day and relating it to the catchment area. Precipitation was measured using eight automatic tipping bucket rain gauges calibrated to measure cumulative rainfall every 10 min with a 0.2 mm resolution (five tipping bucket rain gauges: Theodor Friedrichs, Schenefeld, Germany, and three weather stations: ECRN-100 high-resolution rain gauge). Using Thiessen polygons, we estimated the weighted contribution of rainfall of every tipping bucket in each catchment. A more detailed description of the study sites and instrumentation can be found in Jacobs, Weeser, et al. (2018). Turbidity was measured in situ as a surrogate for suspended sediment concentrations using a ultraviolet/visible (UV/Vis) spectroscopy sensor (spectro::lyser, s::can Messtechnik GmbH, Vienna, Austria). Turbidity is measured in formazin turbidity unit (FTU) by transmitting a beam of light to an optical receptor. With an increase in water turbidity the transmission of light decreases. To calculate sediment concentrations, a site-specific turbidity-suspended sediment calibration was established (section 2.3.1). Before each turbidity measurement, the window of the sensors was automatically cleaned by compressed air to remove any interfering particles. The sensors were additionally cleaned manually on a weekly basis using a specific cleaning agent recommended by the manufacturer to reduce biofouling on the measurement window and by manually removing debris and sediment.

Figure 2. (a–c) Incised and unpaved tracks provide a direct connection with the stream, (d and e) degraded and disturbed riverbank from livestock entering the streams, and (f) eroded suspended sediments in streams within the smallholder agriculture catchment.

2.3. Calibration, Quality Assurance, and Analysis

2.3.1. Sediment-Turbidity Rating Curve

We used a site-specific, ex situ incremental suspension calibration to convert long-term turbidity records into an estimate of instantaneous suspended sediment concentrations (mg L^{-1}). A river water-sediment suspension with 16 to 18 concentration increments was established to simulate changing stream water suspended sediment concentrations occurring from low flow conditions (minimum 0 mg L^{-1}) to storm events (maximum 4,607 mg L^{-1}). The sediment suspension consisted of fine suspended sediment collected from sediment traps (time-integrated Phillips samplers) and fine soil material mixed with turbid river water collected during storm events. To ensure that only the clay size fraction remained in the suspension, the sediment suspension was decanted twice after the settling time for coarse particles (particle size >2 μm) had elapsed (Stokes law: 98 s). The spectro::lyser probes from each monitoring station measured each concentration increment starting with river water representing low flow conditions (0 to 8 FTU). Small quantities of the synthetic sediment suspension were added at each concentration increment until the maximum measurable turbidity of 1,500 FTU was reached. The exact concentration was then determined gravimetrically from a 250 ml subsample at each increment. Total suspended sediment (TSS) load was determined by multiplying suspended sediment concentration by discharge. Suspended sediment yield was calculated by integrating the sediment load over time and relating it to the catchment area. The sediment mass is reported in tonnes (t = Mg) to conform with other published values.

2.3.2. Data Quality Assurance

Quality assurance of the turbidity, discharge, and precipitation data set was performed in two different ways. First, during equipment maintenance and manually downloading of the data any observed anomalies were recorded in a log book. Potential causes of anomalous values included (i) sensor above water level, (ii) turbidity sensor completely buried by deposited sediment during storm periods, (iii) biofilm or other

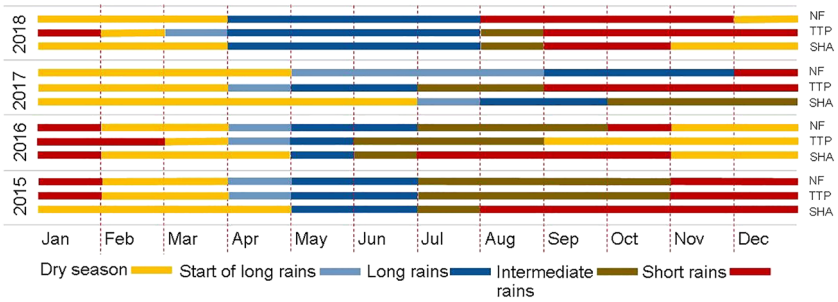

Figure 3. Timing of the five hydrological seasons for the natural forest (NF), tea-tree plantation (TTP), and smallholder agriculture (SHA) catchment during the observation period January 2015–December 2018.

phenomena on the measurement window due to malfunctioning of automatic cleaning with compressed air, (iv) measurement gaps due to incidents of power supply failure, or (v) counting of number of tips by the rain gauges restricted by blocked funnel or spiderwebs. The readings for these periods were flagged with Not-a-Number (NaN).

After anomalous values were replaced by NaN, the median absolute deviation (MAD) was used to detect local outliers. The MAD has the following form:

$$MAD_i = b\, M_{i2}(|x_i - M_{i1}(x_i)|) \tag{1}$$

where x_i is the whole data set, M_{i1} is the median of the data set, and M_{i2} is the median of the absolute deviation from the data set from its median. The constant b estimates the standard deviation and was set to 1.4826 for normal distribution (Leys et al., 2013).

A moving window of k measurements around observation x_i at time t_i was used to detect local outliers with $x_j = (x_{i-k/2} \ldots x_{i-1}, x_{i+1} \ldots x_{i+k/2})$:

$$\frac{x_i - M_{j,\,i}}{MAD_{j,\,i}} > a \tag{2}$$

where $a = 6$ is the threshold for outlier selection, $M_{j,i}$ is the median, and the $MAD_{j,\,i}$ is the MAD for x_j, while the moving window k was set to 16. Missing sediment data were interpolated using a linear function.

2.3.3. Data Analysis

All data were tested for normality with the Shapiro-Wilk test. We tested significant differences on suspended sediment, rainfall, and discharge values among the different land uses using Kruskal-Wallis test for analyses of variances. To detect the significance of the effect of land use on the hydrological and sedimentological parameters, and within and among seasons on suspended sediment load, we used the pairwise Wilcoxon rank sum test.

Five seasons, dry season, start of long rains, long rains (long rainy season), intermediate rains (season between the long and short rainy season), and short rains (short rainy season), were identified to calculate their contribution to annual suspended sediment yield (Jacobs, Weeser, et al., 2018). The periods were chosen based on exceeding a threshold of monthly specific discharge for each catchment. The seasons for each year vary in length and timing due to variations in the onset of the rains and monthly streamflow (Figure 3).

2.3.4. Modeling Flow Pathways

A linear continuous-time (CT) transfer function (TF) model with rainfall-runoff nonlinearity was used to identify the dynamics that explain the response of water flow pathways to rainfall within a catchment by conceptualizing a *Single-Input, Single-Output* (SISO) system (Young & Garnier, 2006). These types of models are equivalent to systems of linear differential equations and can be applied in numerous mass and energy transport as well as chemical or biochemical process applications, including flow and sediment delivery models (Chappell et al., 2006). The TF modeling process follows the *Data-Based Mechanistic* (DBM) modeling philosophy, searching through a range of model structures, ordering them according to statistical criteria, then retaining models that have a physical explanation (Young & Beven, 1994). The DBM approach

produces parsimonious models describing rainfall-runoff relationships that include very few tunable parameters (Lees, 2000). Hourly time series of rainfall (mm hr^{-1}) was used as input and the corresponding hourly time series of discharge (m^3 s^{-1}) as output (the units conversion is absorbed into the model coefficients, in case of Equation 6—into coefficient b_0). These parameters have hydrological interpretation, describing hydrological pathways, so while these are not strictly hydrological models derived from the process models, they still apply to hydrological systems (Beven, 2012).

Hydrological processes are known to be nonlinear (Beven, 2012), with the effectiveness of rainfall (amount of rainfall converted into discharge) dependent upon the state of saturation of the catchment. Therefore, the rainfall-runoff nonlinearity is modeled using the Hammerstein model structure, with the input (rainfall) transformed using a nonlinear function into what is termed "effective rainfall," which then drives the linear dynamics of the transport process model. This study uses a power law relationship between measured rainfall and effective rainfall as surrogate for soil moisture to translate rainfall to effective rainfall (see Text S1 in the supporting information for more details). Effective rainfall is the dynamically changing proportion of rainfall representing the volume of streamflow generated after soil moisture storage is deducted from the total rainfall (Beven, 2012). The RIVCBJ (Refined Instrumental Variable Continuous Time Box-Jenkins Identification, for continuous models, Young & Garnier, 2006) algorithm was used to estimate model parameters. RIVCBJ is a component of the CAPTAIN toolbox, which runs within MATLAB® (Taylor et al., 2007). The linear CT TF model has the following form:

$$Y(s) = \frac{B(s)}{A(s)}U(s)e^{-s\tau} + E(s) \tag{3}$$

$A(s)$ and $B(s)$ characterize the dynamic relationship between the input and the output signals in the Laplace operator domain. The Laplace operator is the Laplace frequency domain equivalent of the time derivative operator $s \sim \frac{d}{dt}$. Functions $A(s)$ and $B(s)$ are constructed as polynomials in the s domain as follows, with m and n being the respective orders of the numerator and denominator polynomials:

$$A(s) = s^n + a_1 s^{n-1} + \ldots + a_n s^0 \tag{4}$$

$$B(s) = b_0 s^{m-1} + b_1 s^{m-2} + \ldots + b_m s^0 \tag{5}$$

In Equation 3 $Y(s)$ denotes the Laplace transform of the output signal as hourly streamflow (m^3 s^{-1}), $U(s)$ is the Laplace transform of the input signal hourly rainfall (mm hr^{-1}), $E(s)$ are the model residuals, and $e^{-s\tau}$ is the Laplace transform of time delay τ representing the pure time delay (as opposed to the dynamic lag resulting from the system's dynamics) in time units between the input and output signals.

In this study, up to third-order models were tested for all the sites and model fit was evaluated according to the coefficient of determination (R_t^2) (also known as the Nash-Sutcliffe efficiency) (see Text S2) and the Young Identification Criterion (YIC) (see Text S3 and S4). First-order TF models were selected for the three catchments, where each system has a different depletion time, determined by its time constant (TC). A first-order CT TF model is written as follows:

$$Y = \left(\frac{b_0}{s + a_1}\right)e^{-s\tau}U = \left(\frac{SSG}{sTC + 1}\right)e^{-s\tau}U \tag{6}$$

where $1/a_1$ is the TC and the parameter b_0/a_1 represent the steady state gain (SSG) of the hypothetical pathway of rainfall through the catchment with a and b as the dynamic response characteristics. The TC reflects the response between the input (rainfall) and the output (runoff or streamflow) (Young & Garnier, 2006). Linear CT TF models were identified for each year between 2015 and 2018 for all three catchments.

2.3.5. Sediment Response to Hydrological Variables

We used the cross-correlation function (CCF) to identify the statistical correlation between two sets of time series at different time lags (Lee et al., 2006; Mayaud et al., 2014). Rainfall and discharge time series were cross correlated with the suspended sediment concentration time series. The peak response time

Table 2
Hydrological Characteristics and Total Suspended Sediment (and 95% Confidence Interval) for the Three Catchments Under Different Land Use Natural Forest (NF; 35.9 km^2), Tea-Tree Plantations (TTPs; 33.3 km^2), and Smallholder Agriculture (SHA; 35.9 km^2) in the South-West Mau, Kenya

Site	Year	Annual rainfall (mm yr^{-1})	Annual specific discharge (mm yr^{-1})	Runoff coefficient[a]	Total suspended sediment load (t yr^{-1})	Total suspended sediment yield (t km^{-2} yr^{-1})
NF	2015	1,986	714 (693–738)	0.36 (0.35–0.37)	407 (378–439)	11.3 (10.5–12.2)
	2016	1,846	518 (497–542)	0.28 (0.27–0.29)	667 (615–724)	18.6 (17.1–20.2)
	2017	1,783	483 (466–502)	0.27 (0.26–0.28)	673 (622–729)	18.7 (17.3–20.3)
	2018	1,755	812 (783–844)	0.46 (0.45–0.48)	1,337 (1,228-1,457)	37.2 (34.2–40.6)
	Mean	1,842 A	632 (610–656) A	0.34 (0.33–0.36) A	771 (711–837) A	21.5 (19.8–23.2) A
TTP	2015	1,928	768 (730–820)	0.40 (0.38–0.43)	2,376 (2,185-2,603)	71.4 (65.6–78.2)
	2016	1,655	593 (555–642)	0.36 (0.34–0.39)	1,397 (1,277-1,539)	42.0 (38.4–46.2)
	2017	1,478	408 (372–468)	0.28 (0.25–0.32)	780 (701–880)	23.4 (21.0–26.4)
	2018	1,858	673 (634–728)	0.36 (0.34–0.39)	1,042 (952–1,151)	31.3 (28.6–34.5)
	Mean	1,730 A	610 (573–665) A	0.35 (0.33–0.38) A	1,399 (1,279-1,543) A	42.0 (38.4–46.3) A
SHA	2015	1,607	561 (539–582)	0.35 (0.34–0.36)	2,324 (2,161-2,494)	85.4 (79.5–91.7)
	2016	1,369	479 (456–503)	0.35 (0.33–0.37)	2,271 (2,088-2,464)	83.5 (76.8–90.6)
	2017	1,416	492 (471–514)	0.35 (0.33–0.36)	2,440 (2,237-2,653)	89.7 (82.2–97.5)
	2018	1,823	953 (920–986)	0.52 (0.50–0.54)	7,273 (6,774-7,790)	267.4 (249.1–286.4)
	Mean	1,554 A	621 (596–646) A	0.39 (0.38–0.41) A	3,577 (3,315-3,851) A	131.5 (121.9–141.6) B

Note. Different capital letters indicate significant differences between the different land uses ($p < 0.05$).
[a]Annual specific discharge as proportion of annual rainfall.

between either precipitation or discharge to sediment concentrations was calculated as the delay time in time lags together with its correlation strength between these variables. CCFs were calculated as follows:

$$CCC(\tau) = \frac{\frac{1}{n}\sum (x_i - \overline{x})(y_{i-\tau} - \overline{y})}{\sigma_x \sigma_y} \quad (7)$$

where $CCC(\tau)$ is the cross-correlation coefficient at time lag τ, $\tau = 0, \pm 1 \pm 2 \ldots \pm m$ between the two time series (sampled every 10 min), where x_i is observed rainfall or positive derivative of discharge at sample number i and $y_{i-\tau}$ is the suspended sediment concentration at sample number $i - \tau$, $\overline{x}$ is the mean rainfall or positive derivative of discharge, $\overline{y}$ is the mean suspended sediment concentration, σ_x is the standard deviation of rainfall or estimated positive derivative of discharge, and σ_y is the standard deviation of suspended sediment and n is the number of data points. At the 95% confidence interval, lag-time correlations are significant when $CCC(\tau)$ exceeds the standard error of $2/\sqrt{N}$, where N is the length of the data set (Diggle, 1990). The positive derivative of discharge, that is, the estimated rate of change on the rising limb of the hydrograph, was selected because the main sediment pulses are mostly generated during the rising limb (Alexandrov et al., 2003; De Girolamo et al., 2015). A similar derivative effect has been observed in dynamic sediment load models by Walsh et al. (2011). The CCF analysis was carried out for each year between 2015 and 2018 for all three catchments.

3. Results

3.1. Hydrological Response of the Three Catchments

Mean annual rainfall for the study period was 1,842, 1,730 and 1,554 mm yr^{-1} with maximum hourly rainfall over the whole observation period of 37.4, 33.1, and 27.5 mm hr^{-1} for the NF, TTPs, and SHA catchments, respectively. The wettest year for the SHA catchment was 2018 with 1,823 mm yr^{-1} of rainfall, while for the NF and TTPs precipitation was highest in 2015 with 1,986 and 1,928 mm yr^{-1}, respectively. The annual mean specific discharge was 632 ± 157, 610 ± 153, and 621 ± 224 mm yr^{-1} for the NF, TTPs, and SHA catchments, respectively. The catchment runoff coefficient was similar for the NF and the TTPs with a mean of 0.34 and 0.35, respectively, and 0.39 for the SHA (Table 2).

Discharge in all catchments was flashy and varied seasonally. Rising limbs were generally steep and had variable falling limbs depending on event size. The highest discharge peaks were measured during the

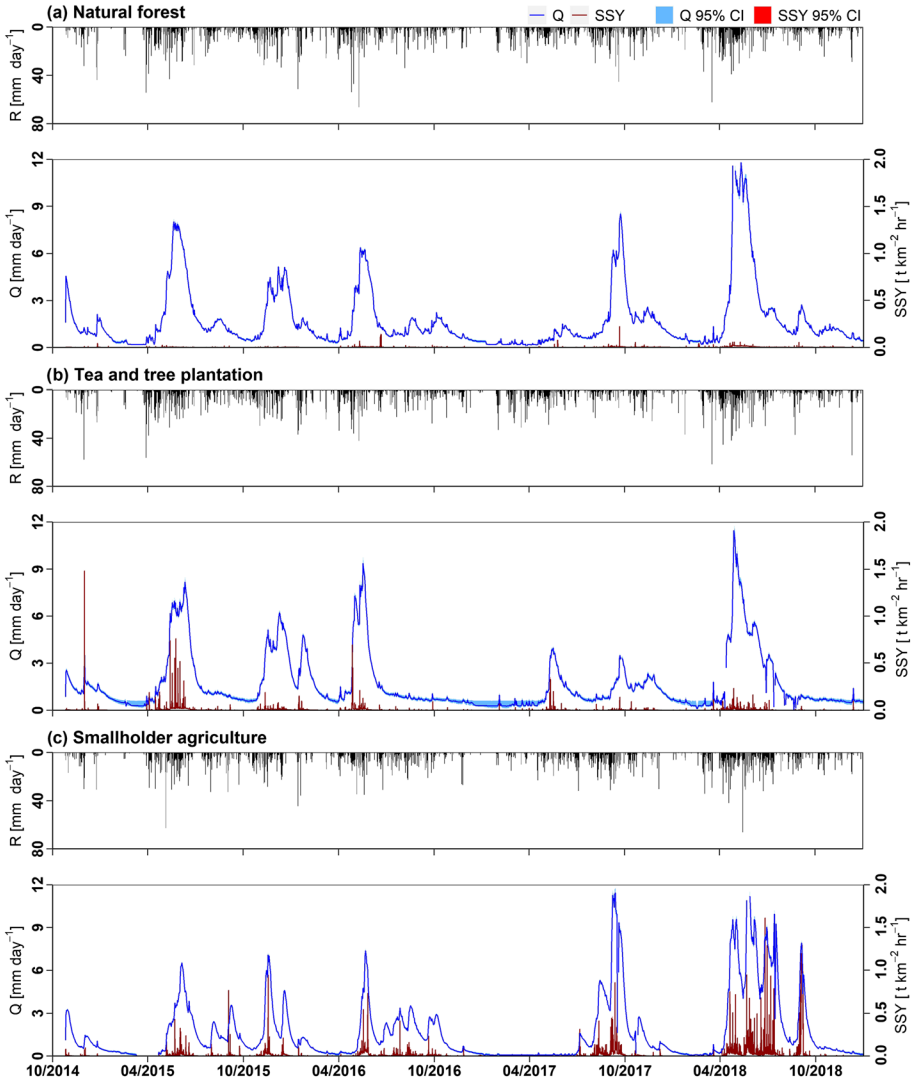

Figure 4. Time series of daily accumulated rainfall (R) (mm day^{-1}), daily specific discharge (Q) (mm day^{-1}) and hourly suspended sediment yield (SSY) (t km^{-2} hr^{-1}) aggregated from 10 min resolution with 95% confidence interval of the (a) natural forest, (b) smallholder agriculture, and (c) tea-tree plantation catchments in the South-West Mau, Kenya, between October 2014 and December 2018.

long rainy seasons between April and July in 2015, 2016, and 2018. In contrast, 2017 was the driest year with a late onset of the rains and the highest discharge peaks between August and November for the SHA and the NF catchments. However, in the TTP catchment the rains started in May lasting until November 2017, resulting in discharge peaking in May and September 2017. High discharges were also recorded in January 2016 because the 2015 rains continued through November and December and were followed by an unusually wet January (Figure 4).

3.2. Relationship Between Turbidity and Suspended Sediment Concentration

We obtained one rating curve for all three catchments to predict suspended sediment concentration from the measured turbidity values. A linear model provided the best fit between the in situ turbidity and suspended sediment concentrations, and there was no significant difference between slopes for each site-specific calibration (p value > 0.1). The intercept of the linear model was forced through the origin to prevent negative sediment concentrations at low turbidity, yielding an equation of the form TSS = 2.4*turbidity ($R^2 = 0.98$, p value < 0.001, $n = 50$; Figure 5). This equation was used to convert the turbidity data to suspended sediment concentrations.

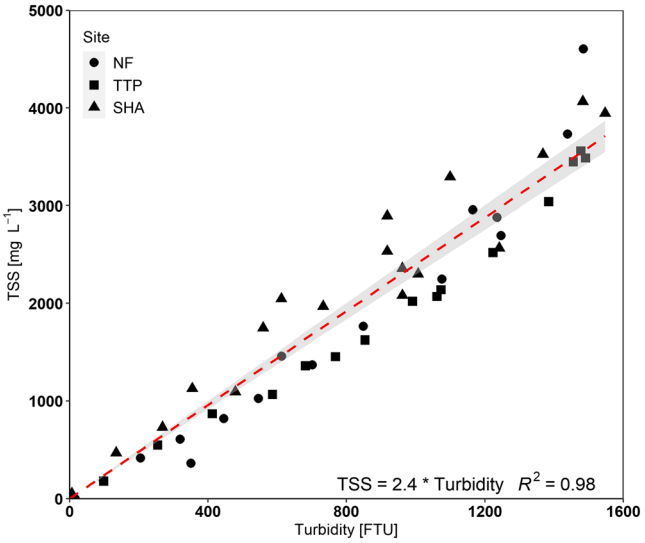

Figure 5. Relation between total suspended sediment concentrations (TSS) (mg L^{-1}) and turbidity (FTU = formazin turbidity unit) measurements for three catchments: natural forest (NF), tea-tree plantations (TTPs), and smallholder agriculture (SHA) and the fitted linear model (gray shaded area: 95% confidence interval).

3.3. Suspended Sediment Dynamics

Sediment yield for the NF was lower than for the other two catchments (Figure 4). The sedigraph of the NF had smaller peaks with a short event time, whereas the SHA and TTPs showed a steep increase followed by a flat recession with a long event time. The sedigraph of the SHA catchment showed a flashy sediment response to rainfall and increased discharge. The maximum sediment yield in the NF catchment was 0.2 t km^{-2} hr^{-1}, followed by the TTPs with 1.5 t km^{-2} hr^{-1} and the SHA with a maximum sediment peak of 1.6 t km^{-2} hr^{-1} (Figure 4). The mean annual suspended sediment yield was significantly higher for the SHA catchment (131.5 ± 90.6 t km^{-2} yr^{-1}) than for the TTPs (42.0 ± 21.0 t km^{-2} yr^{-1}) and the NF (21.5 ± 11.1 t km^{-2} yr^{-1}) ($p < 0.05$) (Table 2). The lowest mean suspended sediment concentration (33.8 ± 73.8 mg L^{-1}) was also lowest for the NF catchment, followed by the TTPs (47.4 ± 90.7 mg L^{-1}). Concentrations were 3 to 4 times higher at the outlet of the SHA catchment (128.6 ± 233.4 mg L^{-1}) than at the other catchments ($p = 0.04$). The daily mean suspended sediment load from the NF was the lowest, followed by the TTPs and the SHA (2.1, 3.9 and 10.0 t day^{-1}, respectively). The TSS load for the entire study period (2015–2018) for the SHA (14,308 t) was 4 times higher than that of the NF (3,083 t), whereas sediment load for the TTPs (5,595 t) was only twice that of the NF. These loads represent a mean of 771, 1,399, and 3,577 t yr^{-1} for the NF, TTPs, and SHA, respectively. Suspended sediment yield increased from 2015 to 2018 in the NF and SHA catchments. In the TTPs, a similar sediment and rainfall pattern was observed with a decline from 2015 to 2017 and then an increase again in 2018 (Table 2). The NF had the longest period of missing data lasting for 95 days in November 2015 to February 2016, followed by a shorter gap in the SHA of 50 days from March to April 2015 and the TTPs had the shortest period of missing sediment data of 13 days between March and April 2017. Besides these periods, minor gaps were usually of less than 24 hr with a total of missing sediment data of 7% for the NF, 2% for the TTPs and 4% for the SHA catchments between 2015 and 2018.

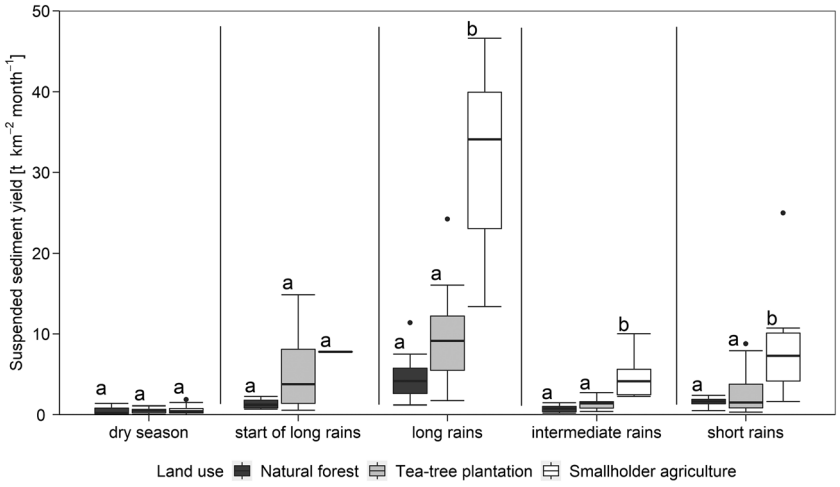

Figure 6. Boxplots of the monthly total suspended sediment yield (t km^{-2} month^{-1}) for different seasons for the natural forest (NF), tea-tree plantations (TTPs), and smallholder agriculture (SHA) catchments in the South-West Mau, Kenya. Seasons: dry season, start of the long rainy season, long rainy season, intermediate rainy season, and short rainy season between January 2015 and December 2018. Different letters above the box plot indicate significant differences between the land uses within each season ($p < 0.05$).

Table 3
Summary of the Linear Continuous-Time Transfer Function Models for the Natural Forest, Tea-Tree Plantation and Smallholder Agriculture Catchment in the South-West Mau, Kenya, for Four Years (Study Period 2015–2018)

Site	Year	Time constant (days)	YIC	R_t^2	Model structure [n, m, τ]
Natural forest	2015	11.5	−11.2	0.92	[1, 1, 2]
	2016	12.6	−11.1	0.92	[1, 1, 2]
	2017	8.4	−11.2	0.92	[1, 1, 2]
	2018	9.8	−12.1	0.93	[1, 1, 2]
Tea-tree plantations	2015	12.1	−10.4	0.86	[1, 1, 2]
	2016	9.6	−11.5	0.90	[1, 1, 2]
	2017	13.0	−8.3	0.54	[1, 1, 2]
	2018	10.5	−11.4	0.92	[1, 1, 2]
Smallholder agriculture	2015[a]	8.6	−10.7	0.86	[1, 1, 2]
	2016	8.7	−11.3	0.88	[1, 1, 3]
	2017	6.2	−12.5	0.96	[1, 1, 2]
	2018	6.9	−11.4	0.92	[1, 1, 2]

Note. YIC = Young Identification Criterion, R_t^2 = coefficient of determination, and model structure [n = denominator polynomial, m = numerator polynomial, and τ = pure time delay].
[a]Data used in the analysis 1 May to 31 December 2015.

3.4. Seasonal Variations in Suspended Sediment

During the study period, suspended sediment yield showed pronounced seasonal variability, with most sediment being transported during the long rains in all catchments, and the highest monthly yields being recorded for the SHA catchment (Figure 6). Overall, more than half of the sediment yield (45–52%) was attributed to the long rains, which cover less than one third of the year. The sediment contribution during the long rains, intermediate rains, and short rains in the SHA was significantly greater than in the NF and TTPs ($p < 0.05$). For the NF the streams carried significantly more material during the long rains (mean yield of 4.3 ± 1.8 t km^{-2} month^{-1}) than during any other season. In the TTPs and SHA, the sediment yield for the long rains (mean 10.9 ± 6.9 and 30.7 ± 10.6 t km^{-2} month^{-1}, respectively) differed significantly from the dry season (mean 0.4 ± 0.2 and 0.6 ± 0.3 t km^{-2} month^{-1}, respectively), the intermediate rains (mean 1.1 ± 0.6 and 5.4 ± 3.3 t km^{-2} month^{-1}, respectively) and the short rains (mean 3.2 ± 2.2 and 23.9 ± 26.1 t km^{-2} month^{-1}, respectively), while there was no difference between the sediment yield for the start of the long rains (mean 5.7 ± 6.5 and 7.8 t km^{-2} month^{-1}, respectively) and the long rains ($p < 0.05$).

3.5. Flow Pathways and Streamflow Dynamics

We compared hydrological flow pathways for each catchment as these are key in delivering sediments to the streams. Rainfall-runoff response was modeled over a continuous period of one year for each monitoring year 2015–2018 (see Figure S1). In all three catchments, first-order linear models (Equation 6) were selected because these had the highest coefficients of determination (R_t^2) ranging between 86% and 93% and explained the data with the most negative YIC ranging between −12.5 and −10.4. The TTPs had a lower model performance in 2017 compared to the other years with a R_t^2 value of 54% and a YIC of −8.3, where the first-order model was identified as the optimal model (Table 3). A simple first-order model was used to derive the TC to compare the dynamic relationship between rainfall and runoff response among the three catchments. Our interpretation of the CT TF model suggests a slower rainfall-runoff catchment response in the NF and TTP catchments in contrast to the fast flow response to rainfall in the SHA catchment. The TCs calculated ranged from 8.4 to 11.5 days in the NF catchment and from 9.6 to 13.0 days in the TTPs. The SHA had TCs between 6.2 to 8.6 days (Table 3).

Table 4
Summary of Cross-Correlation Functions (CCFs) Between Rainfall/Positive Derivative of Discharge to Suspended Sediment With Time Lag (in Hours) and Peak Cross-Correlation Coefficients Reported for the Natural Forest, Tea-Tree Plantation, and Smallholder Agriculture Catchment in the South-West Mau, Kenya, Over Four Years (Study Period 2015–2018)

		Discharge to sediment		Rainfall to sediment	
Site	Year	Time lag (hours)	CCF coefficient	Time lag (hours)	CCF coefficient
Natural forest	2015[a]	1.0	0.10	1.5	0.16
	2016[a]	<0.2	0.03	<0.2	0.05
	2017	0.5	0.07	<0.2	0.12
	2018	0.5	0.10	0.2	0.03
Tea-tree plantations[b]	2015	2.5	0.34	1st 0.5 and 2nd 6.5	1st 0.08 and 2nd 0.17
	2016	2.3	0.18	1st 1.0 and 2nd 7.0	1st 0.08 and 2nd 0.16
	2017	3.2	0.32	1st 0.8 and 2nd 8.5	1st 0.08 and 2nd 0.14
	2018	1st 0.5 and 2nd 2.0	1st 0.17 and 2nd 0.17	1st 0.3 and 2nd 5.0	1st 0.18 and 2nd 0.15
Smallholder agriculture	2015	2.8	0.27	0.7	0.13
	2016	2.2	0.18	1.5	0.08
	2017	3.8	0.17	1.5	0.11
	2018	2.2	0.21	3.5	0.15

[a]Data used in the analysis 1 January to 22 November 2015 and 1 to 31 December 2016. [b]The 1st and 2nd identify the first and second time lag and CCF coefficient of the CCF in the tea-tree plantation.

Water Resources Research

10.1029/2020WR027495

Table 5
Overview of Different Studies Reporting Annual Suspended Sediment Yields (SSY) in Kenyan Headwater Streams and Tropical Montane Forest Catchments Worldwide Derived From Gauging Station Measurements

Montane catchment	Area (km^2)	Land use	Study period (year)	Annual rainfall ($mm\ yr^{-1}$)	SSY ($t\ km^{-2}\ yr^{-1}$)	Reference
Subcatchments of Sondu Basin (West Kenya)	35.9	Natural forest	2014–2018	1,842	21	This study
	33.3	Tea-tree (eucalyptus) plantations	2014–2018	1,730	42	
	27.2	Smallholder agriculture	2014–2018	1,554	131	
Different catchments throughout southern half of Kenya	n.a.	Natural forest (100%)	1948–1968	n.a.	20–30	Dunne (1979)
	n.a.	Natural forest (>51%)	1948–1968	n.a.	10–100	
	n.a.	Agricultural land (>50%)	1948–1968	n.a.	10–1,500	
	n.a.	Grazing land	1948–1968	n.a.	5,000–20,000	
Athi (Kenya)	510	Agriculture, grazing land, and settlements	1985	n.a.	109	Kithiia (1997)
Upper Mara-Emarti (South-West Kenya)	2,450	Smallholder agriculture and urban development	2011–2014 (3–4 months)	1,400	33	Dutton et al. (2018)
Middle Mara-Talek (South-West Kenya)	4,050	Grazing land	2011–2014 (3–4 months)	600	44	Dutton et al. (2018)
Ruharo (Uganda)	2,121	Grazing land, agriculture, and <20% Papyrus wetlands	2009–2010	1,535	106	Ryken et al. (2015)
Koga (Uganda)	379	Grazing land, agriculture, and >80% Papyrus wetlands	2009–2010	1,330	37	Ryken et al. (2015)
Andit Tid (Ethiopia)	4.77	Agriculture (30%)	1989–1996	1,467	522	Guzman et al. (2013)
Anjeni (Ethiopia)	1.13	Agriculture (80%)	1989–1996	1,675	2,470	
Maybar (Ethiopia)	1.12	Agriculture (60%)	1989–2001	1,417	740	
May Zegzeg (Ethiopia)	1.87	Agriculture and grazing land	2000	774	850	Nyssen et al. (2009)
		Agriculture and grazing land with soil conservation practices	2006	708	190	
Arvorezinha (South Brazil)	1.23	Agriculture with traditional soil management and natural forest	2002–2003	2,051	298	Minella et al. (2018)
		Agriculture with soil conservation practices and natural forest	2004–2008	1,655	68	
		Agriculture with traditional soil management and cultivated forest	2009–2016	2,102	163	
Conceição (South Brazil)	800	>85% agriculture (soybean, wheat, oats, and ryegrass) with soil management, <15% gallery forest, wetlands, and urban areas	2000–2010	1,718	140	Didoné et al. (2014)
			2011	1,422	242	
			2012	1,463	41	
Guaporé (South Brazil)	2,000	Agriculture (soybean, tobacco, maize, oats, and ryegrass), grazing land, and cultivated forest	2000–2010	1,550	140	Didoné et al. (2014)
			2011	1,195	390	
			2012	1,660	158	
Baru (Borneo)	0.44	Disturbed logged natural forest	1989	3,205	1,632	Douglas et al. (1993)
		Natural forest immediately after logging	1991	2,609	1,017	Douglas et al. (1993)
		Natural forest after logging	1995–1996	2,956	592	Chappell et al. (2004)
W8S5 (Borneo)	1.7	Natural forest	1989	3,205	118	Douglas et al. (1993)
			1991	2,609	117	
Mae Sa (Thailand)	74.2	Natural forest (62%) and agriculture (>20%)	2006–2008	1,743	323	Ziegler et al. (2014)
Basper (Philippines)	0.32	Grassland and shrubs	2013	2,660	2,740	Zhang et al. (2018)

Note. n.a. = no data available.

3.6. Time Lags Between Rainfall and Discharge to Sediment Concentrations

The analysis using CCFs (Equation 7) showed statistically significant correlations between rainfall and discharge to suspended sediment exceeding the 95% confidence interval of 0.001 for a sample size of 61,201 in all three catchments for the four years. The CCF indicates the impulse response time between the peak of rainfall and discharge to the suspended sediment peak (see Figure S2). The NF had almost instantaneous (<10 min) to rapid responses (1.5 hr) in suspended sediment to both rainfall and discharge in all four years. A period shorter than a year was used for the NF in 2015 and 2016 because of missing sediment data (Table 4). The rainfall to sediment cross correlogram in the TTPs differed from the other two catchments, with a first fast peak within 1 hr followed by a delayed second peak after 5 to 8.5 hr. The discharge to sediment response in the TTPs was similar to that of the SHA catchment with a time lag of around 2 to 3 hr. The SHA had variable time lags between either rainfall or discharge to sediment ranging between 1.5 and 3.8 hr. The impulse response time between the peaks of discharge and sediment concentration was in general longer compared to the rainfall peak (Table 4).

4. Discussion

4.1. Suspended Sediment Dynamics

This study shows that the annual suspended sediment yield is around 6 times greater for the drier SHA catchment and twice greater in the TTP catchment compared to the wetter NF catchment. The sediment yield difference is likely the result of more vegetation cover and low surface hydrological connectivity in the NF, where consequently erosion processes (including mass wasting) are not as active. Similar findings were reported for the neighboring Mara River Basin, where a semiarid catchment had higher suspended sediment yields (44 t km^{-2} yr^{-1}) with half of the annual rainfall in contrast to a wetter but less populated and less disturbed catchment (33 t km^{-2} yr^{-1}) (Dutton et al., 2018) (Table 5).

Missing sediment data and linear interpolation to fill these gaps could have increased the uncertainty in the sediment yields calculated. However, data gaps during dry periods, such as those in the sediment data for the NF during 2015 and 2016, would not have a large influence on yield calculations because of the small amount of material transported. Gaps during periods of heavy rainfall, which occasionally occurred in the SHA catchment due to siltation, could have contributed to underestimation of the sediment yield, as peaks in the sediment concentration could be missing.

For Africa, suspended sediment yield was estimated to be 634 t km^{-2} yr^{-1} at continental scale based on 682 catchments and rivers with larger drainage areas (mean >1,000 km^2) (Vanmaercke et al., 2014). Compared to this, and other sediment studies in Kenya with varying catchment sizes of 24–42,000 km^2 and 8.2 to 6,330 t km^{-2} yr^{-1} (Dunne, 1979; Vanmaercke et al., 2014), our annual suspended sediment yields (21–131 t km^{-2} yr^{-1}) are within the lower reported ranges. Suspended sediment yields from the TTPs and NF catchment of our study are comparable to those observed in the neighboring upper Mara river basin (33 t km^{-2} yr^{-1}; Dutton et al., 2018), which is dominated by small-scale farming and urban development. The SHA catchment in our study had slightly higher suspended sediment yields than the Athi catchment in Kenya (109 t km^{-2} yr^{-1}; Kithiia, 1997) and had lower suspended sediment yields than disturbed agricultural catchments in montane headwaters such as the May Zegzeg catchment in Ethiopia (850 t km^{-2} yr^{-1}; Nyssen et al., 2009) or the Arvorezinha, Conceição, and Guapore catchments in South Brazil (140–298 t km^{-2} yr^{-1}; Didoné et al., 2014; Minella et al., 2018). Guzman et al. (2013) found that in Ethiopia the highest suspended sediment yields (2,470 t km^{-2} yr^{-1}) in small catchments were in those with the largest proportion of agricultural land. Their reported annual yields were significantly higher than the suspended sediment yields observed in this study with similar annual rainfall. Annual suspended sediment yields of 117 up to 2,740 t km^{-2} yr^{-1} from undisturbed to highly disturbed forest or upland grassland catchments were measured in Southeast Asia (Borneo, Thailand, and the Philippines) subjected to mass wasting during typhoon or posttyphoon events (Douglas et al., 2014; Ziegler et al., 2014).

4.2. Factors Controlling Sediment Yield

4.2.1. Vegetation Cover

The low annual suspended sediment yield measured in the Mau forest shows that forest vegetation is the most effective surface cover to limit soil erosion despite the steepest slopes of the forested

catchment (Table 1). The dense vegetation, diverse strata, and complex rooting systems prevent soil detachment and trap potentially erodible material. Similarly, a dense perennial tea vegetation covers the soil surface in the TTPs, which can buffer erosive rainfall (Edwards & Blackie, 1979). Nevertheless, the annual suspended sediment yield for the TTP catchment was twice that of the NF despite the soil conservation practices applied by tea companies such as mulching and planting of buffer strips (oat grass) between rows of young tea bushes or cover trees on newly planted tea plots. This indicates that high sediment loads originate from unprotected bare surfaces during renovation of tea plantations or logging activities of woodlots. Logging activities trigger overland flow and erosion processes and lead sediments to the streams, when there are no buffer strips (Chappell et al., 2004; Douglas et al., 1993). The dense vegetation contrasts with the land management in the SHA catchment, where steep slopes tend to be bare between crop harvest and the start of the next cropping season. During that period, bare surfaces are prone to soil erosion, although cropland surface erosion was not observed, which may be explained by the high infiltration rates previously measured on these croplands (401 ± 211 mm hr^{-1}) (Owuor et al., 2018). The routing of main flow paths was observed on compacted gullied tracks, which act as ephemeral channels during a storm event. Based on these observations, we hypothesize that rural unpaved tracks in the SHA generate a larger contribution to the total sediment load than agricultural land, but further work is required to confirm this. A potential reason for the annual increase in suspended sediment yield in the SHA and the NF catchments during the study period could be the reduced tree cover and increasing areas under annual crops and forest disturbance indicated by the study of Brandt et al. (2018).

4.2.2. Connectivity Between Sediment Sources and the Streams

The TTPs and the SHA have higher catchment surface connectivity than the NF, which may be causing higher sediment transfer by connecting multiple source areas with the streams. Lateral linkages (tracks, gullies, or drains) connect sediment source areas at catchment scale with the stream network (Lane & Richards, 1997), which can be an important driving force for the total sediment load into the rivers (Sidle & Ziegler, 2010).

In the SHA catchment, unpaved tracks are the main pathways for people and livestock to access streams, thus being frequently used and heavily trafficked also by motorbikes (Figure 2). This activity generates highly compacted surfaces, where soil infiltration is impeded. Ziegler et al. (2001) observed that unpaved rural roads, similar in appearance to the unpaved tracks of our study, generate significantly more overland flow compared to adjacent hillslopes. As a consequence of low infiltration rates and downslope-orientated tracks, surface runoff energy increases generating more volume and velocity of flow that can transport large quantities of soil, eventually eroding tracks into gullies (Sidle & Ziegler, 2010; Svoray & Markovitch, 2009). Other researchers found a strong influence of subsurface water tables in valleys on gully formation and the development of large-scale sediment mobilization (Tebebu et al., 2010; Zegeye et al., 2018). High sediment loads at the outlet of the SHA catchment are thought to originate from the eroded unpaved tracks and its connecting adjacent source areas. Catchment drainage density is higher in the SHA (0.64 km km^{-2}) compared to the NF and TTPs (0.48 and 0.42 km km^{-2}, respectively) suggesting a link to increased erosion rates. The TTP catchment is hydrologically connected through a network of tracks and well-engineered paved and unpaved drains in between the tea fields. The design of the well-engineered drains took into account the appropriate routing of surface runoff to the riparian zones before entering the streams, suggesting a higher hydrological connectivity than in the SHA catchment. However, the drains are well maintained with a densely forested riparian zone, which reduces sediment export, thereby reducing sediment transport connectivity. The strong hydrological connectivity of the TTP catchment could lead to high sediment transport and loads with poor maintenance of the drainage network.

4.2.3. Riparian Zones

Dense riparian vegetation can trap sediments before they reach the stream (Pavanelli & Cavazza, 2010). An intact forested riparian zone in the NF and a riparian buffer of 30 m, as predescribed by the Kenya's Water Act (Kenya, 2012), of mixed indigenous vegetation in the TTPs seem to be reducing sediment delivery to the streams by trapping eroded soil. In contrast, high sediment loads are expected in the SHA catchment, where the riparian vegetation is highly degraded or replaced by crops or woodlots planted on the river banks. Small floodplains in a steep, narrow valley floor provide limited space for sediment storage. In the same river basin, other studies reported that highly degraded riparian zones adjacent to areas cultivated by SHA lead to

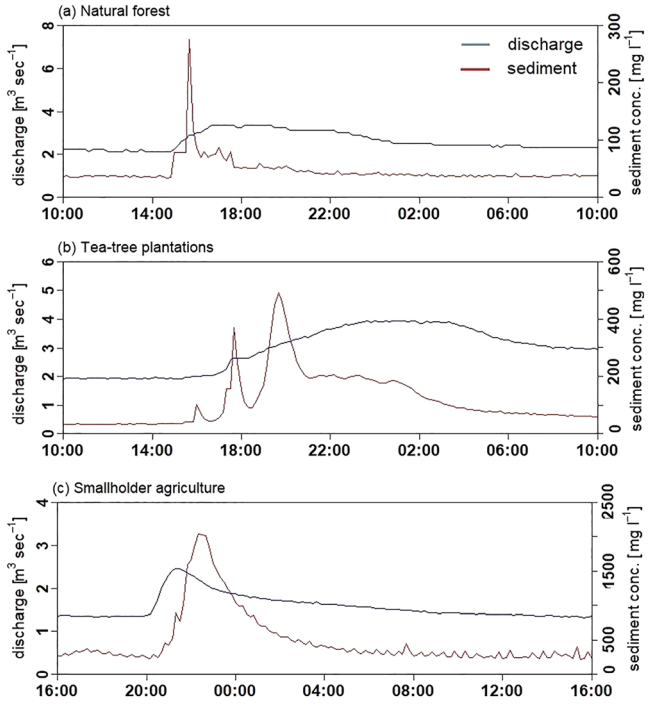

Figure 7. Typical shape of the sedigraph (sediment conc. = concentration [mg L^{-1}]) and hydrograph (discharge [m^3 s^{-1}] [10 min resolution]) for events in the natural forest (2–3 June 2018, 10:00), the tea-tree plantation (24–25 April 2018, 10:00) and the smallholder agriculture (17–18 May 2018, 16:00) catchment in the South-West Mau, Kenya.

increased suspended sediment concentrations (Masese et al., 2012; Njue et al., 2016). In the SHA catchment, livestock access the streams through the riparian area for watering (Figures 2d–2f), which damages the riverbank and the riparian vegetation and further increases sediment supply.

4.3. Water Pathways Are Key for Sediment Production

Hydrological pathways such as surface runoff or subsurface flow are key in determining sediment response in catchments. Our analysis showed that the NF and TTP catchments, with lower suspended sediment yields, had the longest streamflow response time to rainfall using the CT TF model (Equation 6). This supports our hypothesis that shorter pathways indicate that surface runoff mobilizes soil particles causing six times more suspended sediment yields.

The number of pathways and their response time depends on catchment characteristics (Chappell et al., 2006; Ockenden & Chappell, 2011). Forest ecosystems are generally characterized by complex catchment behavior (Chappell et al., 1999), where soils with high infiltration rates promote infiltration to deeper subsurfaces. These pathways can be divided into shallow water pathway and deep groundwater pathway (Chappell & Franks, 1996). The high infiltration rates (760 $\pm$ 500 mm hr^{-1}, Owuor et al., 2018) and the long TCs derived through modeling for the NF catchment (Table 3) point to subsurface flow pathways. Jacobs, Timbe, et al. (2018) reported the occurrence of shallow to deeper subsurface flow by using an endmember mixing analysis in the same NF catchment. Groundwater seemed to be an important stream water source (Jacobs, Timbe, et al., 2018), which agrees with the long response time we calculated (Table 3). Our findings corroborate those of other studies in tropical forest catchments, which demonstrated that subsurface flow is the main water pathway of forest ecosystems (Boy et al., 2008; Muñoz-Villers & McDonnell, 2013; Noguchi et al., 1997). Consequently, low suspended sediment yields are associated with limited surface erosion and sediment delivery to the streams in the NF catchment.

The main pathways in the TTPs with slightly shorter TCs (Table 3) and almost half the infiltration rate (430 $\pm$ 290 mm hr^{-1}, Owuor et al., 2018) compared to the NF suggest that shallow subsurface flow and surface runoff may dominate. Overland flow was observed to be routed through the well-engineered drainage network along roads and surface water drains between tea plantations to the well-buffered fluvial network. Overland flow was also thought to be significant by Jacobs, Weeser, et al. (2018), where nitrate concentrations in stream water seemed to be diluted by surface runoff. The well-maintained drains explain the lower suspended sediment yields, despite the prevalence of surface runoff observed in the TTPs.

The analysis of the SHA catchment showed a relatively fast pathway. However, Owuor et al. (2018) measured infiltration rates of 401 $\pm$ 211 mm hr^{-1} on croplands in the catchment, suggesting that subsurface flow is the most likely pathway. Nevertheless, field observations of runoff along with poorly maintained highly compacted tracks, and the shape of a classification of hysteresis loops by Jacobs, Weeser, et al. (2018) provides a contrasting insight suggesting that surface runoff in the SHA is an important vector for sediment. Our hypothesis is that the tracks act as ephemeral streams and receive water from the surrounding areas as shallow lateral flow, thus explaining the shorter water response times. The NF and TTP catchment with high tree cover showed similar TCs, whereas the much lower tree cover in the SHA catchment lead to faster pathways. The generally slow pathway component in each model can be explained by the presence of deep and well-drained soils in all catchments (Sombroek et al., 1982).

4.4. Sediment Response Times and Event Duration

The shorter time lag between the peaks of rainfall to sediment than to discharge can be attributed to exposed and easy erodible material adjacent to the outlet. The almost instantaneous sediment response to rainfall in the NF and TTPs suggests sediment supply from readily available, nearby sediment sources

(De Girolamo et al., 2015; Francke et al., 2014; Tena et al., 2014) (Figure 7). Near-channel or in-channel sediment sources can originate from the stream bank or the stream bed (Chappell et al., 1999; Kronvang et al., 1997; Lenzi & Marchi, 2000). Temporarily stored sediment is thought to be mobilized very quickly during the first stages of a storm event (Eder et al., 2010). Fast response systems of short duration and low mass magnitude, as those observed in the NF catchment, are characterized by rapid sediment flushing and fast depletion of sediment supply (Chappell et al., 1999), due to limited availability of eroded material from the protected surface (De Girolamo et al., 2015; Fan et al., 2012; Fang et al., 2008). The paved drain network in the TTP catchment can act as conduits transporting sediment instantaneously from nearby logged plantations or tracks to the stream. The delayed sediment response after a rainfall event in the SHA and the second sediment response in the TTP catchment suggest a long travel distance between the sediment source and the catchment outlet. The delayed response can be related to the magnitude of mass, where more distant sediment source areas from the wider catchment accumulate more mass over a longer period. These responses may also indicate the breaching of barriers such as hedges, fences, or grazing land, especially in the SHA catchment. The long recession limb in the SHA and the TTP catchments is typically explained as a slow depletion of sediment supply (De Girolamo et al., 2015; Francke et al., 2014; Tena et al., 2014). The more pronounced sedigraph in the SHA catchment can be associated with the wide range of accumulated sediment source areas (Figure 7).

4.5. Seasonal Variability of Suspended Sediment

Throughout the study period, we observed distinct seasonal variability in suspended sediment yield for the NF, TTPs, and SHA with higher yields in periods of high discharge and rainfall. In climates with strong seasonality of rainfall, seasons can explain sediment dynamics (De Girolamo et al., 2015; Horowitz, 2008), as we observed in this study. Wet seasons or high-flow events generate the largest proportion (80–95%) of the annual sediment load, as observed by De Girolamo et al. (2015), Sun et al. (2016) and Vercruysse et al. (2017) in other areas, while the sediment load is the smallest in the dry season with less than 5% in our study. The seasonal differences were more pronounced in the SHA catchment compared to the other two catchments explained by the high catchment surface connectivity and low vegetation cover.

5. Conclusions

This study presents the first long-term high-resolution sediment data set in Kenya. The four years of continuous data for the NF, TTP, and SHA catchments provide critical insights in contrasting sediment dynamics of the tropical montane Mau Forest Complex. The analysis revealed that land use is a critically important driver for sediment supply, where SHA generates 6 times more annual suspended sediment yield than a catchment dominated by NF. Besides vegetation cover, a strong catchment surface connectivity through unpaved tracks and gullies from hillslopes to the fluvial network is thought to be the main reason for the differences in sediment yields. However, further work is required to test this hypothesis. Catchments with a high tree cover, such as the NF and the TTPs, seem to have similar water pathways with a dominance of subsurface flow. In contrast, in the highly disturbed landscape such as that of the SHA catchment, surface runoff dominates and soil erosion increases suspended sediment yield. This superficial water pathway results in the more pronounced seasonal impact of rainfall in the SHA compared to the other two catchments, also due to varying vegetation cover. Delayed sediment response to rainfall and a slow depletion in sediment supply in the SHA and TTPs suggests that the wider catchment area is supplying sediment from a range of sediment sources, especially in the catchment dominated by smallholder farming. In contrast, the fast depletion in sediment supply in the NF suggests the importance of nearby sediment sources and temporarily stored sediment.

Land scarcity and population growth bring enormous pressure on NF ecosystems. Forest conversion will increase sediment production, which will affect not only many people in the Sondu River basin who rely on the rivers for drinking water but also Lake Victoria which is already affected by increased sediment supply. The implementation of catchment management, such as soil conservation measures and better engineering of rural trackways, is essential to reduce sediment supply to water bodies. However, a detailed sediment source fingerprinting analysis is necessary to identify the main contributing sediment sources. This will support the application of better management strategies at the source to prevent sediment entering the stream network. Sediment yields reported in other sediment studies in montane SHA catchments were

higher than in our study, which provide a warning of potentially higher sediment loss in the future unless mitigation strategies are implemented.

Data Availability Statement

The raw data are available online (https://dx.doi.org/10.17635/lancaster/researchdata/352) hosted by Lancaster University, UK.

Acknowledgments
We thank the German Federal Ministry for Economic Cooperation and Development (Grant 81206682 "The Water Towers of East Africa: policies and practices for enhancing co-benefits from joint forest and water conservation") and the German Science Foundation (Deutsche Forschungsgemeinschaft DFG Grant BR2238/23-1) for providing financial support for this research. This work was also partially funded by the CGIAR program on Forest, Trees and Agroforestry led by the Centre for International Forestry Research (CIFOR). We would like to thank the tea companies, the Kenya Forest Service (KFS), and the chief of the smallholder agriculture catchment (Kuresoi sublocation) for supporting our research activities and Naomi K. Njue for maintenance of the equipment. Finally, we are also grateful for the valuable and constructive comments from the Associate Editor and three anonymous reviewers.

References

Alexandrov, Y., Laronne, J. B., & Reid, I. (2003). Suspended sediment concentration and its variation with water discharge in a dryland ephemeral channel, northern Negev Israel. *Journal of Arid Environments*, *53*(1), 73–84. https://doi.org/10.1006/jare.2002.1020

Beven, K. J. (2012). *Rainfall-runoff modelling: The primer* (2nd ed.). Chichester, UK: Wiley-Blackwell. https://doi.org/10.1002/9781119951001

Binge, F. W. (1962). *Geology of the Kericho area* (pp. 2–73). Kenya: Ministry of commerce, Industry and Communications, Geological Survey of Kenya.

Boy, J., Valarezo, C., & Wilcke, W. (2008). Water flow paths in soil control element exports in an Andean tropical montane forest. *European Journal of Soil Science*, *59*(6), 1209–1227. https://doi.org/10.1111/j.1365-2389.2008.01063.x

Brandt, P., Hamunyela, E., Herold, M., de Bruin, S., Verbesselt, J., & Rufino, M. C. (2018). Sustainable intensification of dairy production can reduce forest disturbance in Kenyan montane forests. *Agriculture, Ecosystems and Environment*, *265*, 307–319. https://doi.org/10.1016/j.agee.2018.06.011

Brown, T., Schneider, H., & Harper, D. (1996). *Multi-scale estimates of erosion and sediment yields in the Upper Tana basin, Kenya*, *Erosion and Sediment Yield: Global and regional perspectives* (Vol. 236, pp. 49–54). Exeter, UK: IAHS Publ. https://iahs.info/uploads/dms/iahs_236_0049.pdf

Bruijnzeel, L. A. (2004). Hydrological functions of tropical forests: Not seeing the soil for the trees? *Agriculture, Ecosystems and Environment*, *104*(1), 185–228. https://doi.org/10.1016/j.agee.2004.01.015

Chappell, N. A., Douglas, I., Hanapi, J. M., & Tych, W. (2004). Sources of suspended sediment within a tropical catchment recovering from selective logging. *Hydrological Processes*, *18*(4), 685–701. https://doi.org/10.1002/hyp.1263

Chappell, N. A., & Franks, S. (1996). Property distributions and flow structure in the Slapton Wood Catchment. *Field Studies*, *8*, 698–718.

Chappell, N. A., McKenna, P., Bidin, K., Douglas, I., & Walsh, R. P. D. (1999). Parsimonious modelling of water and suspended sediment flux from nested catchments affected by selective tropical forestry. *Philosophical Transactions of the Royal Society B Biological Sciences*, *354*(1391), 1831–1846. https://doi.org/10.1098/rstb.1999.0525

Chappell, N. A., Tych, W., Chotai, A., Bidin, K., Sinun, W., & Chiew, T. H. (2006). BARUMODEL: Combined data based mechanistic models of runoff response in a managed rainforest catchment. *Forest Ecology and Management*, *224*(1–2), 58–80. https://doi.org/10.1016/j.foreco.2005.12.008

De Girolamo, A. M., Pappagallo, G., & Lo Porto, A. (2015). Temporal variability of suspended sediment transport and rating curves in a Mediterranean river basin: The Celone (SE Italy). *Catena*, *128*, 135–143. https://doi.org/10.1016/j.catena.2014.09.020

Didoné, E. J., Minella, J. P. G., Reichert, J. M., Merten, G. H., Dalbianco, L., de Barrros, C. A. P., & Ramon, R. (2014). Impact of no-tillage agricultural systems on sediment yield in two large catchments in Southern Brazil. *Journal of Soils and Sediments*, *14*, 1287–1297. https://doi.org/10.1007/s11368-013-0844-6

Diggle, P. (1990). *Time series: A biostatistical introduction* (5th ed.). Oxford, UK: Clarendon Press.

Douglas, I., Greer, T., Bidin, K., & Sinun, W. (1993). *Impact of roads and compacted ground on post-logging sediment yield in a small drainage basin, Sabah, Malaysia*, *Hydrology of Warm Humid Regions* (Vol. 216, pp. 213–218). Yokohama Symposium: IAHS Publ.

Dunne, T. (1979). Sediment yield and land use in tropical catchments. *Journal of Hydrology*, *42*(3–4), 281–300. https://doi.org/10.1016/0022-1694(79)90052-0

Dutton, C. L., Subalusky, A. L., Anisfeld, S. C., Njoroge, L., Rosi, E. J., & Post, D. M. (2018). The influence of a semi-arid sub-catchment on suspended sediments in the Mara River, Kenya. *PLoS ONE*, *13*, 1–19. https://doi.org/10.1371/journal.pone.0192828

Eder, A., Strauss, P., Krueger, T., & Quinton, J. N. (2010). Comparative calculation of suspended sediment loads with respect to hysteresis effects (in the Petzenkirchen catchment, Austria). *Journal of Hydrology*, *389*(1–2), 168–176. https://doi.org/10.1016/j.jhydrol.2010.05.043

Edwards, K. A., & Blackie, J. R. (1979). The Kericho research project. *East African Agricultural and Forestry Journal*, *43*, 44–50. https://doi.org/10.1080/00128325.1979.11662941

Fan, X., Shi, C., Zhou, Y., & Shao, W. (2012). Sediment rating curves in the Ningxia-Inner Mongolia reaches of the upper Yellow River and their implications. *Quaternary International*, *282*, 152–162. https://doi.org/10.1016/j.quaint.2012.04.044

Fang, H., Chen, H., Cai, Q., & Huang, X. (2008). Effect of spatial scale on suspended sediment concentration in flood season in hilly loess region on the Loess Plateau in China. *Environmental Geology*, *54*(6), 1261–1269. https://doi.org/10.1007/s00254-007-0908-2

Foster, I. D. L., Rowntree, K. M., Boardman, J., & Mighall, T. M. (2012). Changing sediment yield and sediment dynamics in the Karoo Uplands, South Africa; Post-European impacts. *Land Degradation & Development*, *23*(6), 508–522. https://doi.org/10.1002/ldr.2180

Foy, R. H., & Bailey-Watts, A. E. (1998). Observations on the spatial and temporal variation in the phosphorus status of lakes in the British Isles. *Soil Use and Management*, *14*(s4), 131–138. https://doi.org/10.1111/j.1475-2743.1998.tb00631.x

Francke, T., Werb, S., Sommerer, E., & López-Tarazón, J. A. (2014). Analysis of runoff, sediment dynamics and sediment yield of sub-catchments in the highly erodible Isábena catchment, Central Pyrenees. *Journal of Soils and Sediments*, *14*(12), 1909–1920. https://doi.org/10.1007/s11368-014-0990-5

Fraser, A. I., Harrod, T. R., & Haygarth, P. M. (1999). The effect of rainfall intensity on soil erosion and particulate phosphorus transfer from arable soils. *Water Science and Technology*, *39*(12), 41–45. https://doi.org/10.2166/wst.1999.0527

Fryirs, K. (2013). (Dis)connectivity in catchment sediment cascades: A fresh look at the sediment delivery problem. *Earth Surface Processes and Landforms*, *38*(1), 30–46. https://doi.org/10.1002/esp.3242

Gellis, A. C., & Mukundan, R. (2013). Watershed sediment source identification: Tools, approaches, and case studies. *Journal of Soils and Sediments*, *13*(10), 1655–1657. https://doi.org/10.1007/s11368-013-0778-z

Githui, F., Gitau, W., Mutua, F., & Bauwens, W. (2009). Climate change impact on SWAT simulated streamflow in western Kenya. *International Journal of Climatology*, *29*(12), 1823–1834. https://doi.org/10.1002/joc.1828

Grangeon, T., Legout, C., Esteves, M., Gratiot, N., & Navratil, O. (2012). Variability of the particle size of suspended sediment during highly concentrated flood events in a small mountainous catchment. *Journal of Soils and Sediments*, *12*(10), 1549–1558. https://doi.org/10.1007/s11368-012-0562-5

Guzman, C. D., Tilahun, S. A., Zegeye, A. D., & Steenhuis, T. S. (2013). Suspended sediment concentration–discharge relationships in the (sub-) humid Ethiopian highlands. *Hydrology and Earth System Sciences*, *17*(3), 1067–1077. https://doi.org/10.5194/hess-17-1067-2013

Hilton, J., O'Hare, M., Bowes, M. J., & Jones, J. I. (2006). How green is my river? A new paradigm of eutrophication in rivers. *Science of the Total Environment*, *365*(1–3), 66–83. https://doi.org/10.1016/j.scitotenv.2006.02.055

Horowitz, A. J. (2008). Determining annual suspended sediment and sediment-associated trace element and nutrient fluxes. *Science of the Total Environment*, *400*(1–3), 315–343. https://doi.org/10.1016/j.scitotenv.2008.04.022

ISRIC (2007). *Soil and terrain database for Kenya (KENSOTER), version 2.0, at scale 1:1 million (KENSOTER)*. Wageningen, The Netherlands: World Soil Information.

Jacobs, S. R., Timbe, E., Weeser, B., Rufino, M. C., Butterbach-Bahl, K., & Breuer, L. (2018). Assessment of hydrological pathways in East African montane catchments under different land use. *Hydrology and Earth System Sciences*, *22*(9), 4981–5000. https://doi.org/10.5194/hess-22-4981-2018

Jacobs, S. R., Weeser, B., Guzha, A. C., Rufino, M. C., Butterbach-Bahl, K., Windhorst, D., & Breuer, L. (2018). Using high-resolution data to assess land use impact on nitrate dynamics in East African tropical montane catchments. *Water Resources Research*, *54*, 1812–1830. https://doi.org/10.1002/2017WR021592

Kemp, P., Sear, D., Collins, A., Naden, P., & Jones, I. (2011). The impacts of fine sediment on riverine fish. *Hydrological Processes*, *25*(11), 1800–1821. https://doi.org/10.1002/hyp.7940

Republic of Kenya (2012). *Water Act, laws of Kenya, Chapter 372* (2nd ed., pp. 1–245). Nairobi, Kenya: National Council for Law Reporting with the Authority of the Attorney-General.

Kithiia, M. S. (1997). *Land use changes and their effects on sediment transport and soil erosion within the Athi drainage basin, Kenya*, *Human impact on erosion and sedimentation* (Vol. 245, pp. 145–150). Rabat, Morocco: IAHS Publ.

Krhoda, G. O. (1988). The impact of resource utilization on the hydrology of the Mau Hills Forest in Kenya. *Mountain Research and Development*, *8*(2/3), 193. https://doi.org/10.2307/3673447

Kronvang, B., Laubel, A., & Grant, R. (1997). Suspended sediment and particulate phosphorus transport and delivery pathways in an arable catchment, Gelbæk stream Denmark. *Hydrological Processes*, *11*(6), 627–642. https://doi.org/10.1002/(SICI)1099-1085(199705)11:6<627::AID-HYP481>3.0.CO;2-E

Lane, S. N., & Richards, K. S. (1997). Linking river channel form and process: Time, space and causality revisited. *Earth Surface Processes and Landforms*, *22*(3), 249–260. https://doi.org/10.1002/(SICI)1096-9837(199703)22:3<249::AID-ESP752>3.0.CO;2-7

Lee, L. J. E., Lawrence, D. S. L., & Price, M. (2006). Analysis of water-level response to rainfall and implications for recharge pathways in the Chalk aquifer, SE England. *Journal of Hydrology*, *330*(3–4), 604–620. https://doi.org/10.1016/j.jhydrol.2006.04.025

Lees, M. J. (2000). Data-based mechanistic modelling and forecasting of hydrological systems. *Journal of Hydroinformatics*, *2*(1), 15–34. https://doi.org/10.2166/hydro.2000.0003

Lefrançois, J., Grimaldi, C., Gascuel-Odoux, C., & Gilliet, N. (2007). Suspended sediment and discharge relationships to identify bank degradation as a main sediment source on small agricultural catchments. *Hydrological Processes*, *21*(21), 2923–2933. https://doi.org/10.1002/hyp.6509

Lenzi, M. A., & Marchi, L. (2000). Suspended sediment load during floods in a small stream of the Dolomites (northeastern Italy). *Catena*, *39*(4), 267–282. https://doi.org/10.1016/S0341-8162(00)00079-5

Lewis, J. (1996). Turbidity-controlled suspended sediment sampling for runoff-event load estimation. *Water Resources Research*, *32*(7), 2299–2310. https://doi.org/10.1029/96WR00991

Leys, C., Ley, C., Klein, O., Bernard, P., & Licata, L. (2013). Detecting outliers: Do not use standard deviation around the mean, use absolute deviation around the median. *Journal of Experimental Social Psychology*, *49*(4), 764–766. https://doi.org/10.1016/j.jesp.2013.03.013

Masese, F. O., Raburu, P. O., Mwasi, B. N., & Etiégni, L. (2012). Effects of deforestation on water resources: Integrating science and community perspectives in the Sondu-Miriu River Basin Kenya. *New Advance Contribution to Research InTechnology*, 3–18.

Mayaud, C., Wagner, T., Benischke, R., & Birk, S. (2014). Single event time series analysis in a binary karst catchment evaluated using a groundwater model (Lurbach system, Austria). *Journal of Hydrology*, *511*(100), 628–639. https://doi.org/10.1016/j.jhydrol.2014.02.024

Minella, J. P. G., Clarke, R. T., Merten, G. H., & Walling, D. E. (2008). *Sediment source fingerprinting: testing hypotheses about contributions from potential sediment sources*, *Sediment dynamics in changing environments* (Vol. 325, pp. 31–37). Christchurch, New Zealand: IAHS Publ.

Minella, J. P. G., Merten, G. H., Barros, C. A. P., Ramon, R., Schlesner, A., Clarke, R. T., et al. (2018). Long-term sediment yield from a small catchment in southern Brazil affected by land use and soil management changes. *Hydrological Processes*, *32*(2), 200–211. https://doi.org/10.1002/hyp.11404

Mogaka, H., Gichere, S., Davis, R., & Hirji, R. (2006). *Climate variability and water resources degradation in Kenya: Improving water resources development and management* (Vol. 69). Washington, DC USA: World Bank.

Morgan, R. P. C. (2005). *Soil erosion and conservation* (3rd ed., pp. 1–316). Cranfield University, UK: Blackwell Publishing Ltd.

Morris, G. L. (2014). Sediment management and sustainable use of reservoirs. In *Modern Water Resources Engineering* (pp. 279–337). Totowa, NJ: Humana Press.

Muñoz-Villers, L. E., & McDonnell, J. J. (2013). Land use change effects on runoff generation in a humid tropical montane cloud forest region. *Hydrology and Earth System Sciences*, *17*(9), 3543–3560. https://doi.org/10.5194/hess-17-3543-2013

Njue, N., Koech, E., Hitimana, J., & Sirmah, P. (2016). Influence of land use activities on riparian vegetation, soil and water quality: An indicator of biodiversity loss, South West Mau forest Kenya. *Open Journal Finder*, *06*, 373–385. https://doi.org/10.4236/ojf.2016.65030

Noguchi, S., Nik, A. R., Kasran, B., Tani, M., Sammori, T., & Morisada, K. (1997). Soil physical properties and preferential flow pathways in tropical rain forest, Bukit Tarek, Peninsular Malaysia. *Journal of Forest Research*, *2*(2), 115–120. https://doi.org/10.1007/BF02348479

Ntiba, M. J., Kudoja, W. M., & Mukasa, C. T. (2001). Management issues in the Lake Victoria watershed. *Lakes & Reservoirs: Research and Management*, *6*(3), 211–216. https://doi.org/10.1046/j.1440-1770.2001.00149.x

Nyssen, J., Clymans, W., Poesen, J., Vandecasteele, I., De Baets, S., Haregeweyn, N., et al. (2009). How soil conservation affects the catchment sediment budget—A comprehensive study in the north Ethiopian highlands. *Earth Surface Processes and Landforms*, *34*(9), 1216–1233. https://doi.org/10.1002/esp.1805

Nyssen, J., Poesen, J., Moeyersons, J., Deckers, J., Haile, M., & Lang, A. (2004). Human impact on the environment in the Ethiopian and Eritrean highlands—A state of the art. *Earth-Science Reviews*, *64*(3–4), 273–320. https://doi.org/10.1016/S0012-8252(03)00078-3

Ockenden, M. C., & Chappell, N. A. (2011). Identification of the dominant runoff pathways from data-based mechanistic modelling of nested catchments in temperate UK. *Journal of Hydrology*, *402*(1–2), 71–79. https://doi.org/10.1016/j.jhydrol.2011.03.001

Ogden, F. L., Crouch, T. D., Stallard, R. F., & Hall, J. S. (2013). Effect of land cover and use on dry season river runoff, runoff efficiency, and peak storm runoff in the seasonal tropics of Central Panama. *Water Resources Research*, *49*, 8443–8462. https://doi.org/10.1002/2013WR013956

Owens, P. N., Batalla, R. J., Collins, A. J., Gomez, B., Hicks, D. M., Horowitz, A. J., et al. (2005). Fine-grained sediment in river systems: Environmental significance and management issues. *River Research and Applications*, *21*(7), 693–717. https://doi.org/10.1002/rra.878

Owuor, S. O., Butterbach-Bahl, K., Guzha, A. C., Jacobs, S., Merbold, L., Rufino, M. C., et al. (2018). Conversion of natural forest results in a significant degradation of soil hydraulic properties in the highlands of Kenya. *Soil and Tillage Research*, *176*, 36–44. https://doi.org/10.1016/j.still.2017.10.003

Pavanelli, D., & Cavazza, C. (2010). River suspended sediment control through riparian vegetation: A method to detect the functionality of riparian vegetation. *CLEAN - Soil, Air, Water*, *38*, 1039–1046. https://doi.org/10.1002/clen.201000016

Pellikka, P., Clark, B., Hurskainen, P., Keskinen, A., Lanne, M., Masalin, K., et al. (2004). In *Land use change monitoring applying geographic information system in the Taita hills, SE-Kenya* (pp. 1–8). Nairobi, Kenya: African association of Remote Sensing of Environmental.

Poesen, J., Nachtergaele, J., Verstraeten, G., & Valentin, C. (2003). Gully erosion and environmental change: Importance and research needs. *Catena*, *50*(2–4), 91–133. https://doi.org/10.1016/S0341-8162(02)00143-1

Quinton, J. N., Catt, J. A., & Hess, T. M. (2001). The selective removal of phosphorus from soil. *Journal of Environmental Quality*, *30*(2), 538. https://doi.org/10.2134/jeq2001.302538x

Ramos-Scharrón, C. E., & Thomaz, E. L. (2016). Runoff development and soil erosion in a wet tropical montane setting under coffee cultivation. *Land Degradation & Development*, *28*, 936–945. https://doi.org/10.1002/ldr.2567

Ryken, N., Vanmaercke, M., Wanyama, J., Isabirye, M., Vanonckelen, S., Deckers, J., & Poesen, J. (2015). Impact of papyrus wetland encroachment on spatial and temporal variabilities of stream flow and sediment export from wet tropical catchments. *Science of the Total Environment*, *511*, 756–766. https://doi.org/10.1016/j.scitotenv.2014.12.048

Shaw, E. M., Beven, K. J., Chappell, N. A., & Lamb, R. (2011). *Hydrology in practice* (4th ed., pp. 1–543). London and New York: Taylor & Francis.

Sidle, R. C., & Ziegler, A. D. (2010). Elephant trail runoff and sediment dynamics in northern Thailand. *Journal of Environmental Quality*, *39*(3), 871–881. https://doi.org/10.2134/jeq2009.0218

Sombroek, W. G., Braun, H. M. H. & van der Pouw, B. J. (1982). *Exploratory soil map and agro-climatic zone map of Kenya, 1980, scale 1:1,000,000* (E1 ed., pp. 1–60). Kenya: Ministry of Agriculture - National Agricultural Laboratories.

Sun, L., Yan, M., Cai, Q., & Fang, H. (2016). Suspended sediment dynamics at different time scales in the Loushui River, south-central China. *Catena*, *136*, 152–161. https://doi.org/10.1016/j.catena.2015.02.014

Svoray, T., & Markovitch, H. (2009). Catchment scale analysis of the effect of topography, tillage direction and unpaved roads on ephemeral gully incision. *Earth Surface Processes and Landforms*, *34*(14), 1970–1984. https://doi.org/10.1002/esp.1873

Taylor, C. J., Pedregal, D. J., Young, P. C., & Tych, W. (2007). Environmental time series analysis and forecasting with the Captain toolbox. *Environmental Modelling and Software*, *22*(6), 797–814. https://doi.org/10.1016/j.envsoft.2006.03.002

Tebebu, T. Y., Abiy, A. Z., Zegeye, A. D., Dahlke, H. E., Easton, Z. M., Tilahun, S. A., et al. (2010). Surface and subsurface flow effect on permanent gully formation and upland erosion near Lake Tana in the northern highlands of Ethiopia. *Hydrology and Earth System Sciences*, *14*(11), 2207–2217. https://doi.org/10.5194/hess-14-2207-2010

Tena, A., Vericat, D., & Batalla, R. J. (2014). Suspended sediment dynamics during flushing flows in a large impounded river (the lower River Ebro). *Journal of Soils and Sediments*, *14*(12), 2057–2069. https://doi.org/10.1007/s11368-014-0987-0

Trimble, S. W., & Mendel, A. C. (1995). The cow as a geomorphic agent—A critical review. *Geomorphology*, *13*(1–4), 233–253. https://doi.org/10.1016/0169-555X(95)00028-4

UNEP (2005). *Mau Complex under siege: Continuous destruction of Kenya's largest forest*. Kenya: UNEP.

USGS (2000). *Shuttle Radar Topography Mission (SRTM) 1 arc-second global Reston*. Virginia, USA: U. S. Geological Survey.

Vanmaercke, M., Poesen, J., Broeckx, J., & Nyssen, J. (2014). Sediment yield in Africa. *Earth-Science Reviews*, *136*, 350–368. https://doi.org/10.1016/j.earscirev.2014.06.004

Vanmaercke, M., Zenebe, A., Poesen, J., Nyssen, J., Verstraeten, G., & Deckers, J. (2010). Sediment dynamics and the role of flash floods in sediment export from medium-sized catchments: A case study from the semi-arid tropical highlands in northern Ethiopia. *Journal of Soils and Sediments*, *10*(4), 611–627. https://doi.org/10.1007/s11368-010-0203-9

Vercruysse, K., Grabowski, R. C., & Rickson, R. J. (2017). Suspended sediment transport dynamics in rivers: Multi-scale drivers of temporal variation. *Earth-Science Reviews*, *166*, 38–52. https://doi.org/10.1016/j.earscirev.2016.12.016

Verschuren, D., Johnson, T. C., Kling, H. J., Edgington, D. N., Leavitt, R., Brown, E. T., et al. (2002). History and timing of human impact on Lake Victoria, East Africa. *Royal Society*, *269*(1488), 289–294. https://doi.org/10.1098/rspb.2001.1850

Walling, D. E., & Webb, B. W. (1996). *Erosion and sediment yield: A global overview*, *Erosion and Sediment Yield: Global and regional perspectives* (pp. 1–17). Exeter: IAHS Publ.

Walsh, R. P. D., Bidin, K., Blake, W. H., Chappell, N. A., Clarke, M. A., Douglas, I., et al. (2011). Long-term responses of rainforest erosional systems at different spatial scales to selective logging and climatic change. *Philosophical Transactions of the Royal Society B Biological Sciences*, *366*(1582), 3340–3353. https://doi.org/10.1098/rstb.2011.0054

Wangechi, K. S., Muigai, A. W. T., & Ouma, S. O. (2015). The impact of evolution and socio-economics of commercially exploited fish stock: A review on *Rastrineobola argentea* in Lake Victoria. *Journal of Food Security*, *3*, 82–86. https://doi.org/10.12691/jfs-3-3-3

Wohl, E. (2006). Human impacts to mountain streams. *Geomorphology*, *79*(3–4), 217–248. https://doi.org/10.1016/j.geomorph.2006.06.020

Young, P. C., & Beven, K. J. (1994). Data-based mechanistic modelling and the rainfall-flow non-linearity. *Environmetrics*, *5*(3), 335–363. https://doi.org/10.1002/env.3170050311

Young, P. C., & Garnier, H. (2006). Identification and estimation of continuous-time, data-based mechanistic (DBM) models for environmental systems. *Environmental Modelling and Software*, *21*(8), 1055–1072. https://doi.org/10.1016/j.envsoft.2005.05.007

Zegeye, A. D., Langendoen, E. J., Guzman, C. D., Dagnew, D. C., Amare, S. D., Tilahun, S. A., & Steenhuis, T. S. (2018). Gullies, a critical link in landscape soil loss: A case study in the subhumid highlands of Ethiopia. *Land Degradation & Development*, *29*(4), 1222–1232. https://doi.org/10.1002/ldr.2875

Zhang, J., van Meerveld, H. J. I., Tripoli, R., & Bruijnzeel, L. A. (2018). Runoff response and sediment yield of a landslide-affected fire-climax grassland micro-catchment (Leyte, the Philippines) before and after passage of typhoon Haiyan. *Journal of Hydrology*, *565*, 524–537. https://doi.org/10.1016/j.jhydrol.2018.08.016

Ziegler, A. D., Benner, S. G., Tantasirin, C., Wood, S. H., Sutherland, R. A., Sidle, R. C., et al. (2014). Turbidity-based sediment monitoring in northern Thailand: Hysteresis, variability, and uncertainty. *Journal of Hydrology*, *519*, 2020–2039. https://doi.org/10.1016/j.jhydrol.2014.09.010

Ziegler, A. D., Giambelluca, T. W., Sutherland, R. A., Vana, T. T., & Nullet, M. A. (2001). Horton overland flow contribution to runoff on unpaved mountain roads: A case study in northern Thailand. *Hydrological Processes*, *15*(16), 3203–3208. https://doi.org/10.1002/hyp.480